IEEE Photonics Journal
An IEEE Photonics Society Publication

Open Access

Fiber Bragg Grating Cryosensors for Superconducting Accelerator Magnets

Volume 6, Number 6, December 2014

A. Chiuchiolo
M. Bajko
J. C. Perez
H. Bajas
M. Consales
M. Giordano
G. Breglio
A. Cusano

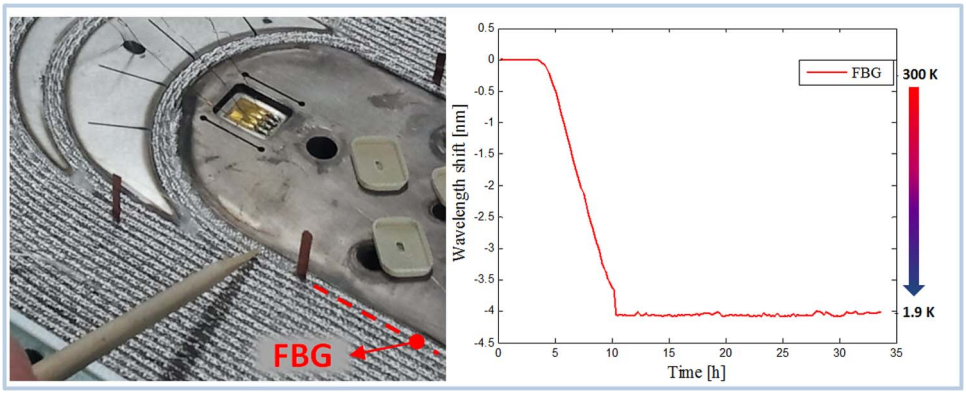

DOI: 10.1109/JPHOT.2014.2343994
1943-0655

Fiber Bragg Grating Cryosensors for Superconducting Accelerator Magnets

A. Chiuchiolo,[1,2] M. Bajko,[2] J. C. Perez,[2] H. Bajas,[2] M. Consales,[1] M. Giordano,[3] G. Breglio,[4] and A. Cusano[1]

[1]Optoelectronic Division, Department of Engineering, University of Sannio, 82100 Benevento, Italy
[2]European Organization for Nuclear Research (CERN), 1211 Genève, Switzerland
[3]Institute for Composite and Biomedical Materials, CNR, 80055 Portici, Italy
[4]Electrical Engineering and Information Technologies Department, University of Naples Federico II, 80138 Napoli, Italy

DOI: 10.1109/JPHOT.2014.2343994

Manuscript received June 19, 2014; revised July 21, 2014; accepted July 23, 2014. Date of publication July 29, 2014; date of current version December 16, 2014. This work was supported by the European Commission through the Transnational Access Activity of the FP7 Research Infrastructures Project EUCARD-2 under Grant 312453. Corresponding author: A. Cusano (e-mail: acusano@unisannio.it).

Abstract: The design, fabrication, and tests of the new generation of superconducting magnets for the High Luminosity upgrade of the Large Hadron Collider (HL-LHC) require the support of an adequate sensing technology able to assure the integrity of the strain-sensitive and brittle superconducting cables through the whole service life of the magnet: assembly up to 150 MPa, cool down to 1.9 K, and powering up to about 16 kA. A precise temperature monitoring is also needed, in order to guarantee the safe working condition of the superconducting cables in the power transmission lines (SC-Link) designed to feed the magnet over long distance. Fiber Bragg Grating–based temperature and strain monitoring systems have been implemented in the first SC-Link prototype and in two subscale dipole magnets and tested in the cryogenic test facility at CERN, at 30 K, 77 K, and 1.9 K.

Index Terms: Fiber optic sensor, FBG, superconducting magnet, superconducting transmission line, strain, cryogenic temperatures.

1. Introduction

The Large Hadron Collider (LHC), the largest circular particle accelerator built at the European Organization for Nuclear Research (CERN), is presently equipped with NbTi based superconducting magnets that achieve a bending field of 8.3 T in the main dipoles. In the framework of the High Luminosity upgrade (HL-LHC), new accelerator magnets able to operate in the 11–13 T range are developed using new design approach for a technology based on Nb_3Sn which has a higher magnetic field capability.

To avoid radiation damage of the power converters presently located in 100 m deep tunnel, it is also planned to bring them to the surface or in radiation-free underground areas feeding the magnets down to the tunnel through High Temperature Superconducting transmission lines (SC-Link) to carry currents up to 20 kA [1]. In this context a complex development phase is required and the implementation of new monitoring systems becomes crucial to provide useful information from fabrication to operation in extreme conditions as ultra-low temperatures (down to 1.9 K), strong electromagnetic fields (up to 13 T), and strong mechanical stress (up to 150 MPa).

To date, resistive sensors are the devices most commonly used for measuring temperature and strain in the field of cryogenic and superconducting magnets, but their sensitivity to the magnetic field and the amount of electrical wires needed for their operation add issues that could be efficiently overcome through the use of Fiber Bragg Grating (FBG) sensors. For their characteristics like small size, lightweight, intrinsic electrical insulation, immunity to electromagnetic interferences and multiplexing capability, FBGs represent an attractive alternative or a complementary instrumentation to the resistive sensors both during the R&D phase and during operation. So far, few studies on the use of FBGs for cryogenic applications and superconducting magnets have been reported in literature mainly limited to a proof of principle of the temperature and strain measurement [2]–[4], but the complex integration in real coils and cryogenic environment still makes this technology not well assessed yet.

This work reports the results of the first FBG integration in the Nb_3Sn coil manufactured at CERN in a dipole configuration and the integration in the first 20 m superconducting link prototype for power transmission lines.

The paper has been organized as follows. Section 2 is dedicated to the working principle of the FBG sensor with a particular interest to the effects of cryogenic temperature on its sensitivity referring to the main results reported in literature.

Section 3 is devoted to the temperature sensors developed for the superconducting transmission lines and tested in wavelength division multiplexing scheme with the goal to monitor the homogeneity of the He gas temperature over long distance. The sensor selection after preliminary studies carried out at CERN and further improvement for the final application is described in Section 3.1. The set up and the integration are detailed in Section 3.2 while the results are discussed in Section 3.3.

Section 4 is dedicated to the strain sensors and the mechanical monitoring of two subscale magnets. In the specific case the strain monitoring is performed both by bonding FBGs on the structure of the magnet and by embedding them in the coil before its impregnation. The challenge of using the FBGs is to embed them directly on the superconducting cables since the coils fabricated at CERN have currently only strain gauges glued on the structure around which the conductor is wound. Section 4.1 is devoted to the description of the set up and the integration in the two magnets and in Section 4.2 the results are discussed giving a global overview of the mechanical behavior of an accelerator magnet during its service life consisting in assembly, cool down and powering.

2. Fiber Bragg Grating Sensors Working Principle

An FBG is a periodic modulation of the index of refraction in the core of an optical fiber formed by exposing the fiber to a UV laser pattern. When broadband light is sent through a Bragg grating, it only reflects the specific wavelength component working like a narrowband reflecting filter. The Bragg reflection wavelength of an FBG is given as

$$\lambda_B = 2n_{eff}\Lambda \tag{1}$$

where n_{eff} is the effective refractive index of the core and Λ is the grating period. The FBG is sensitive to both temperature and strain. The strain response arises from both the physical elongation of the sensor and the change in fiber index because of photo elastic effects. The dependence of the Bragg wavelength on temperature arises from the change of the effective refractive index due to thermo-optic effect and the change of the period due to thermal expansion of the glass [5]. The Bragg wavelength shift with strain (ε) and in temperature (T) can be expressed using

$$\Delta\lambda_B = \lambda_B[(1-\rho_a)\Delta\varepsilon + (\alpha+\xi)\Delta T] \tag{2}$$

where ρ_a is the photo elastic coefficient of the fiber, α is the thermal expansion coefficient and ξ is the thermo-optic coefficient. The temperature sensitivity of the FBG has been previously observed to decrease significantly with decreasing temperature, approaching zero below 50 K [6].

For a bare FBG, the thermal response is dominated by the refractive index change, as the thermal expansion of silica is very low (0.5×10^{-6} at room temperature). Approaching cryogenic temperatures, both the effects reduce, so the temperature sensitivity of a bare FBG dramatically reduces. When the FBG is embedded or bonded, the thermal response is thus dominated by the thermal apparent strain related to the thermal contraction/expansion of the host material offering therefore the possibility of temperature-insensitive strain measurement in cryogenic environments [7].

3. FBGs Based Temperature Monitoring for Superconducting Transmission Lines

The power transmission lines proposed to feed the magnets having a length of approx. 500 m will be made of superconducting cables working at the He gas temperature ranged between 5–30 K. A temperature monitoring is required to keep the temperature homogeneous all along the cryostat in order to assure safe operation of the superconducting cable below its critical temperature (transition temperature from resistive to superconducting state). FBGs read in wavelength division multiplexing scheme give attractive perspectives for the instrumentation wire reduction, but their implementation in cryogenic environment for this application requires a complete study and the selection of the suitable material able to enhance the sensitivity of the FBG in the temperature range of interest.

3.1. Sensors Selection

As previously discussed in Section 2, the FBG's low intrinsic temperature sensitivity at cryogenic temperature requires the development of a cryogenic sensor based on a material selection which aims to use the thermal contraction coefficient (CTE) of the material as temperature dependence parameter [8]. The temperature response of a coated FBG depends on several physical properties of the fiber (thermo—mechanical, thermo optical and elasto-optic effects), on the thermo—mechanical properties of the coating material and on its geometry. The evaluation of the temperature effect on all these parameters in the wide range 4.2–300 K adds complexity to the design and to the selection of the sensor for cryogenic applications.

The CTE of most materials is independent of the temperature below 50 K, in the cases it is not it becomes strongly nonlinear at very low temperature. The Young's modulus of the coating material also plays a crucial role in dominating the bare grating deformation in its own contraction/expansion behavior. Moreover the thickness of the coating is strongly depending on the ability of the elastic modulus to effectively transfer the strain to the optical fiber down to very low temperatures. Nevertheless, besides the behavior of the selected material at cryogenic temperature in terms of CTE and Young's modulus, the manufacture of the sensor can be limited by the adhesion between the material itself and the fiber whether this doesn't assure an homogenous stress distribution at the fiber-coating interface.

Several investigations have been reported in literature on the use of both metals and polymers to improve the FBG sensitivity. Rajini-Kumar *et al.* in [9] show the results of tests carried out on FBGs recoated with aluminum, copper, lead and indium reporting respectively a total wavelength shift of 6.28 nm, 7.08 nm, 9.41 nm, and 10.06 nm at 15 K. Nevertheless the literature highlights the polymers as the best candidate for enhancing the sensitivity of the FBG thanks to their bigger CTE at lower temperature. Few works report that the use of Teflon assures the highest sensitivity achievable inducing a wavelength shift of 19 nm at 77 K [10] however the main inconvenience in using it for coating relies on the difficulties in increasing the adhesion between the substrate and the fiber. The PMMA (polymethyl methacrylate) results to be one of the most affective material among the polymers investigated so far providing a shift of the reflected wavelength of 11.7 at 4.28 K [11]. In light of these studies, similar results have been confirmed and reported in [12] after preliminary investigations carried out in the CERN laboratories where the material selection for the development of a cryogenic FBG based sensor is part of the same research study and becomes essential in finding the most suitable sensor

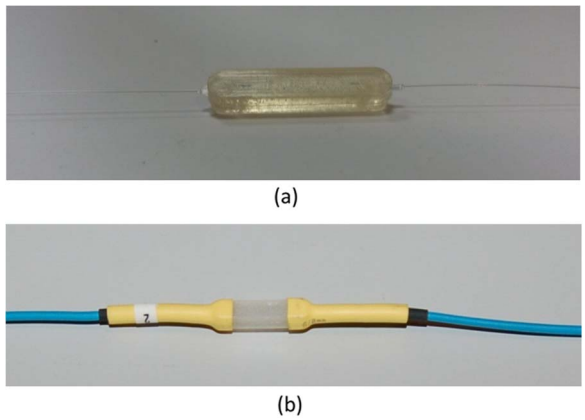

Fig. 1. (a) Epoxy recoated FBG. (b) Customized PMMA recoated FBG with packaging.

responding to the needs and the requirements of the applications described in this work. PMMA and epoxy have been selected and preferred to other coating materials in order to design and test the sensors at 4.2 K and then to further assembly customized arrays for temperature monitoring over long distance. FBG gratings with the following specifications have been coated: 10 mm grating length, Bragg wavelength tolerance ± 0.5 nm, reflectivity $> 90\%$, FWHM (full width at half maximum of the spectrum) < 0.3 nm and reactive casting was used as most suitable manufacturing process to realize the samples. In both PMMA and epoxy samples polymeric precursors highly compatible with silica have been used to enhance the surface wetting before the polymerization. The final nominal dimensions of the Bragg Grating coating were $2.5 \times 5.0 \times 25.0$ mm (height $\times$ width $\times$ length) for both PMMA and epoxy, Fig. 1(a) shows the final result of one FBG recoated with epoxy. Tests on these samples at 4.2 K reported by Esposito *et al.* in [12], show a good feasibility of the manufacturing process and a strong non linearity of the FBG temperature responses especially in the range 10–4.2 K. Nevertheless, besides a further material selection presently on going, samples realized in this way have been considered suitable for the application in the superconducting link prototype, where the range of interest 15–30 K is, so far, well above the range in which the sensor selection has to be improved. However, for the implementation of the selected sensors in customized arrays, an appropriate packaging is needed in order to protect the pigtails from any damage which can occur during the fiber handling and integration in a very complex and harsh environment. Fig. 1(b) shows the packaging of the PMMA recoated FBG with commercial flexible polyolefin heat-shrinking tubes which protect the edges of the sensor.

3.2. Sensors Integration and Set Up

Based on the sensor selection reported above, 8 FBGs of 10 mm long grating, recoated with epoxy and PMMA have been spliced and arranged symmetrically in 4 arrays of 20 m length. The FBGs were placed in proximity of each reference sensor (type CERNOX) in order to monitor the temperature variation in the same locations distributed over the length. The set-up of the FBGs is designed with the aim to continuously monitor the cryostat ambient temperature in order to assure safe working conditions of the superconducting cables during operation. Fig. 2 shows the schematic of the 4 locations where the FBGs and the reference sensors have been placed. The distance of each sensor is considered from the optical interrogator placed more than 20 meters far from the gas entrance. To assure the integrity of the fibers during the installation and the operation, they were placed inside a 10 mm inner diameter Kapton tube, conveniently perforated in order to force the flow of He gas through. The tube was then fixed to the insulated superconducting cable and pushed together with it inside the 20 m long horizontal cryostat.

The first 20 m SC-Link prototype was then cooled to 30 K and the temperature kept homogeneous by a forced flow of He gas coming from a feed box located at the end of the cryostat.

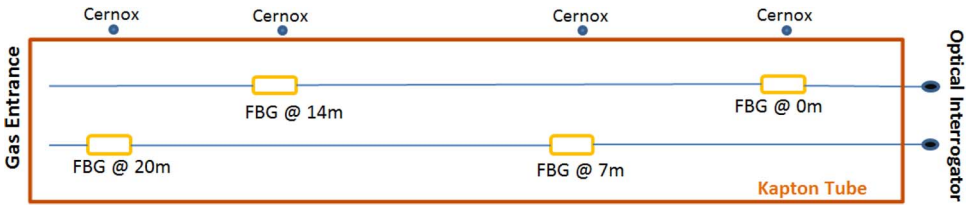

Fig. 2. Schematic of FBGs and Cernox set up in the superconducting link.

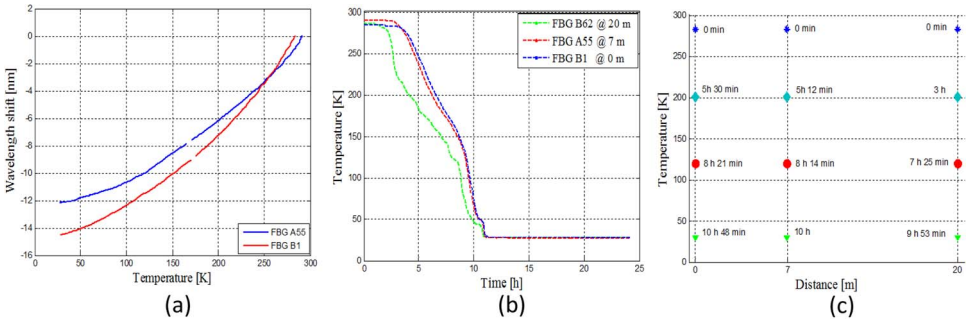

Fig. 3. (a) Epoxy and PMMA recoated sensors characteristic curves $\Delta\lambda$-T. (b) FBGs' temperature profile during cool down from 300 to 30 K. (c) Temperature mapping over the distance of the SC-Link.

The FBGs were connected to the four channels of the Micron Optics sm125 using a dedicated ultra—vacuum tight feed through at the beginning of the cryostat, 25 m away from the feed box where the gas is forced to flow all along the cable.

3.3. Experimental Results

The FBGs reflected wavelengths were continuously monitored during the cool down to 30 K. The sensors are named as FBG A and FBG B to indicate respectively the epoxy and the PMMA recoated ones. Fig. 3(a) shows the typical characteristic curves of the PMMA recoated and the epoxy recoated sensors and the nonlinear behavior of the wavelength with the temperature due to the reduction of the sensitivity with the decreasing temperature, coherently with the expectations already discussed in Section 3.1. For the FBG recoated with PMMA the wavelength shifted by -14.5 nm for the temperature range 300–30 K while the wavelength variation for the FBG recoated with epoxy results to be -12.1 nm in the same temperature range. The dynamics of the fiber optic sensors is clearly depending on the distance from the gas entrance located at 20 m and this is shown in Fig. 3(b) where the FBGs temperature reconstruction during the 12 hours cool down is reported. Coherently with the temperature profile monitored by the reference sensors, it is therefore possible to map the temperature along the cryostat. As shown in Fig. 3(c) a temperature decrease of 85 K is seen at the entrance of the cold gas at 20 m after 3 h while the same temperature is reached at the distance of 7 m and then at the beginning of the cryostat in more than 5 h showing the cooling power of the He gas over long distance. Reaching lower temperature, the time needed to each sensor, therefore to each location, to get the same temperature decreases until the line reaches a stable and homogenous temperature at 30 K in about 12 h. The temperature reconstruction along the 20 m is reported only for 3 of the 4 locations of interest due to a damage occurred to one of the reference sensors during the test.

The capability of the FBGs to monitor the temperature of the He gas along the distance offers the possibility to increase the number of measuring points which cannot be easily implemented with the use of resistive sensors due to the limitation introduced by the wiring. This can also assure the implementation of an FBG based monitoring system able to give redundancy of data helpful in case of fiber or resistive thermometers damages due to the harsh working conditions

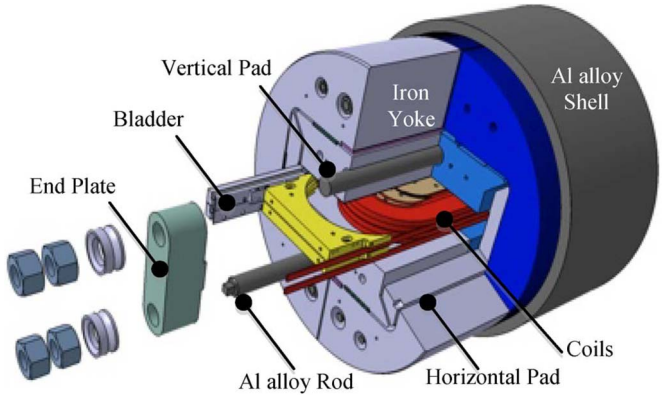

Fig. 4. Magnet structure and main components.

and environment. Moreover, the precise monitoring of the local temperature variation all along the superconducting transmission line gives complementary information to preserve the safe working condition of the cable by detecting eventual leaks which can compromise the homogeneity of the temperature leading, ultimately, to unwanted results in the superconductor in case of a transition from superconducting to resistive state.

4. FBGs Based Strain Monitoring for Superconducting Magnets

The performance of the new generation of accelerator magnets, presently designed, manufactured and tested at CERN, can be strongly affected by the mechanical stress in the windings during magnet operation due to the brittle and strain sensitive characteristics of Nb_3Sn. It is therefore mandatory to understand and to monitor the strain in the superconductor envisaging a precise sensing system both on the support structure of the magnet and inside the coil. For this purpose a strain monitoring system based on FBG sensors have been implemented in two short-scale models of Nb_3Sn dipole magnets: the Short Model Coil (SMC) and Racetrack Model Coil (RMC) magnets. Specifically FBGs have been bonded on the cylindrical Al structure of RMC and embedded in the epoxy impregnated race-track coil of SMC. The schematic of the SMC structure is shown in Fig. 4 [13], [14] (RMC magnet takes over the same design).

During the magnet assembly phase the coil pack is pre-compressed up to 150 MPa through the outside structure in order to retain the electromagnetic forces that appear during the powering. Monitoring the mechanical behavior of the structure is essential in understanding whether the forces become larger than the retaining forces compromising eventually the integrity of the coil during operation [15]. Additionally, the strain monitoring of the coil gives a critical feedback on possible coil motion which may lead to unwanted quenches (transitions from superconducting to conducting state of the material used). The challenge of using the FBG in superconducting magnets is to embed them directly on the superconducting cables where the resistive strain gauges integration is very difficult due to their size.

4.1. Sensors Integration and Set Up

FBGs of 10 mm long grating inscribed in fully polyimide recoated fibers were selected for the integration in the two sub scale dipole magnets. In the specific case of RMC shown in Fig. 5(a), 8 FBGs were arranged in 4 arrays and glued on its structure with standard araldite (two-part adhesive resin) suitable for cryogenic temperature. It is worth to underline that there is not a standard bonding procedure for fiber optic sensors suitable for cryogenic temperatures, so it was chosen to follow the procedure commonly used for the strain gauges at CERN. The interface between the fiber and the structure is an important parameter to consider during the bonding process as the glue adhesion and the layer thickness need to assure the stress transfer from the structure to the sensor without affecting the quality of the FBG reflected signal. For this purpose

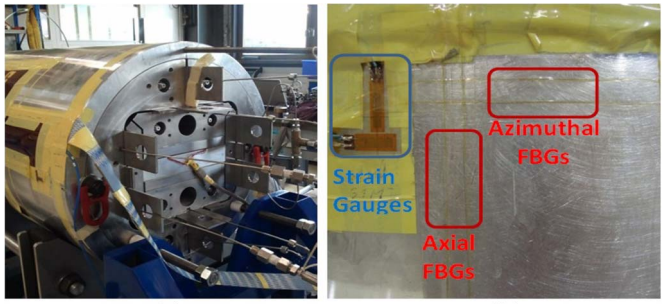

Fig. 5. (a) RMC magnet during assembly. (b) FBGs bonded on RMC Al structure.

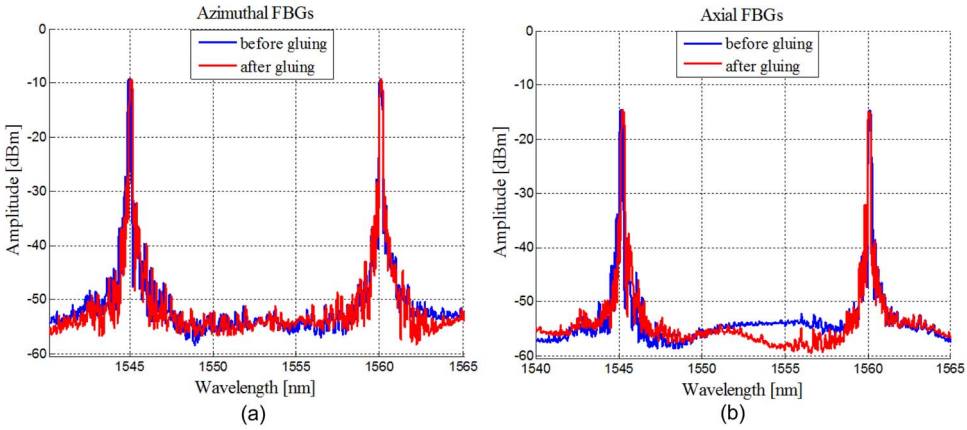

Fig. 6. Reflection spectra of the FBGs glued in the azimuthal and axial directions before and after the bonding process on one side of the magnet.

the bonding process was completed leaving the sensors under pressure for 24 h to minimize the glue thickness between the sensors and the host material. The sensors were placed in transversal and longitudinal directions close to the resistive strain gauges as shown in Fig. 5(b), on two opposite sides of the magnet, where the accumulated stress reaches its peak at high field.

Fig. 6(a) and (b) show the reflection spectra of two FBGs arrays bonded in azimuthal and axial directions before and after the gluing process. The absence of birefringence shows that the bonding layer homogeneously stresses the sensors along their length.

In the SMC coil two single ended FBGs were laid on the winding along its axial direction in its straight part, between the first and the second turn of the winding close to the Ti pole, one for each layer, in a symmetric configuration as shown in the schematic of the transverse cross section in Fig. 7(a). In this location the cable is subjected to the maximum stress during assembly and cool down and the quench location is expected during the powering due to the highest magnetic field in that zone. The coil was also instrumented with voltage taps and resistive strain gauges, glued on the Ti pole as shown in Fig. 7(b). Then the coil was inserted in a mould and impregnated in a vacuum tank using a mix of epoxy resin and polyetheramine hardener at 120 °C [13] as part of the standard fabrication process of the Nb_3Sn coils. The final result of the impregnation of the racetrack coil is shown in Fig. 7(c).

Fig. 8(a) and (b) show the reflection spectra of the two FBGs before and after the impregnation process. The signals are recorded at the same temperature therefore the shift to lower wavelengths obtained after the impregnation process shows the overall longitudinal compression of the sensors due to the compressive stress impressed on them by the composite material.

This compression effect is more evident on FBG1 which shows a shifted wavelength of 280 pm in respect to the 80 pm wavelength shift of FBG2. This difference between the two

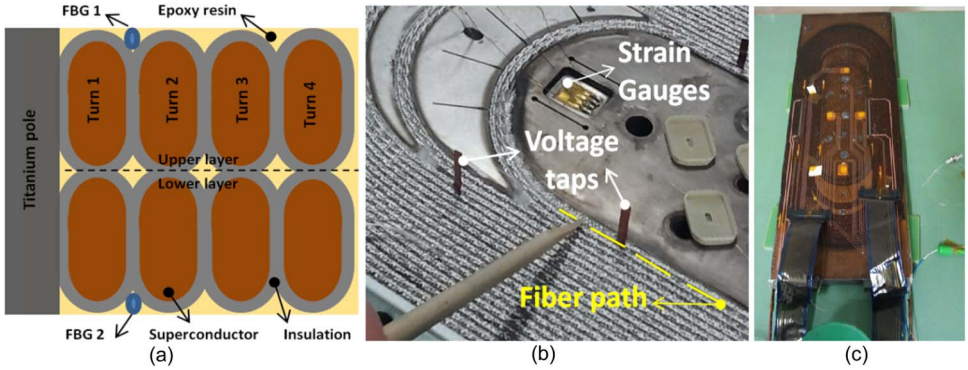

Fig. 7. (a) SMC coil transverse cross section (view from the inside) and FBGs location between the first and the second turn of winding on the upper and lower layer. (b) Location of strain gauges, voltage taps, and fiber. (c) Racetrack coil after impregnation.

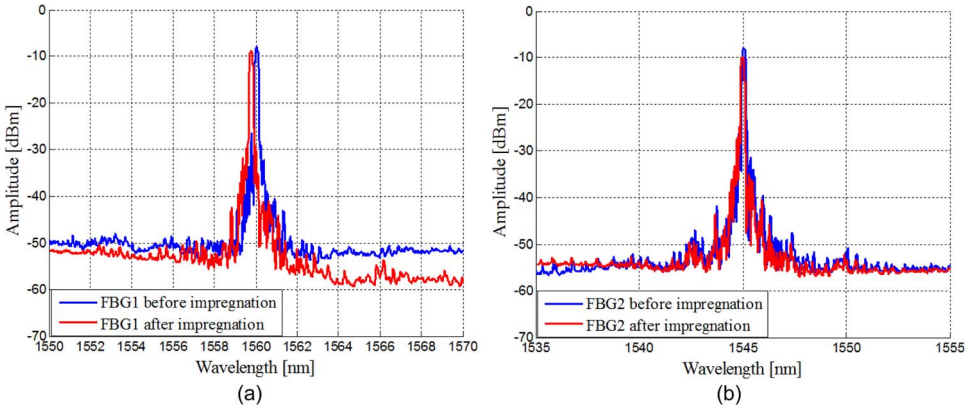

Fig. 8. Reflection spectra of the FBGs and after the embedding process.

sensors can be explained by their different locations and thus the resin thickness surrounding as well as the misalignment of the FBG along its measuring axis.

The magnets were tested in the SM18 test facility at CERN using dedicated vertical cryostats. SMC was tested at 1.9 K temperature, in superfluid He. RMC was tested in a 4 m height cryostat built for LN2 cooling at 77 K in order to study the mechanical properties of the magnets components. The optical fibers were connected through an optic leak—tight feed through at the top of the cryostat to the four channels of the optical interrogator Micron Optics SM125. In the case of RMC it was also used a Micron Optics SM041 Channel Multiplexer connected to the SM125 in order to read the six arrays.

4.2. Experimental Results

The structural behavior of RMC has been monitored during the assembly at room temperature and two thermal cycles at 77 K.

Fig. 9(a) shows the linear behavior of the azimuthal FBG response with the azimuthal strain during the assembly at room temperature, when, by using the bladders and keys technology [16], the shell is gradually set to different pre-stress values in order to deliver the designed pre compression to the coil pack. The strain sensitivity S_ε is found to be 0.7 pm/$\mu\varepsilon$ and 0.8 pm/$\mu\varepsilon$ for the sensors in the azimuthal direction giving coherent strain values measured by the FBGs in respect to the values measured by the resistive strain gauges. On side 1, the FBGs computed strain variation after the assembly results to be 1839 pm/$\mu\varepsilon$ and 1835 pm/$\mu\varepsilon$ in comparison with 1679 pm/$\mu\varepsilon$ measured by the strain gauges. On side 2 the two FBGs measure 1365 pm/$\mu\varepsilon$ and 1388 pm/$\mu\varepsilon$ in

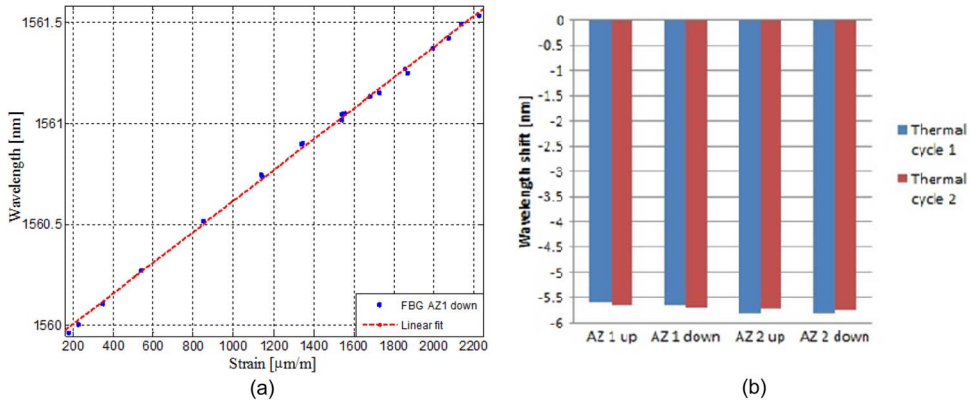

Fig. 9. (a) Azimuthal strain characteristic curve during RMC assembly. (b) Azimuthal wavelength shifts during RMC thermal cycles to 77 K.

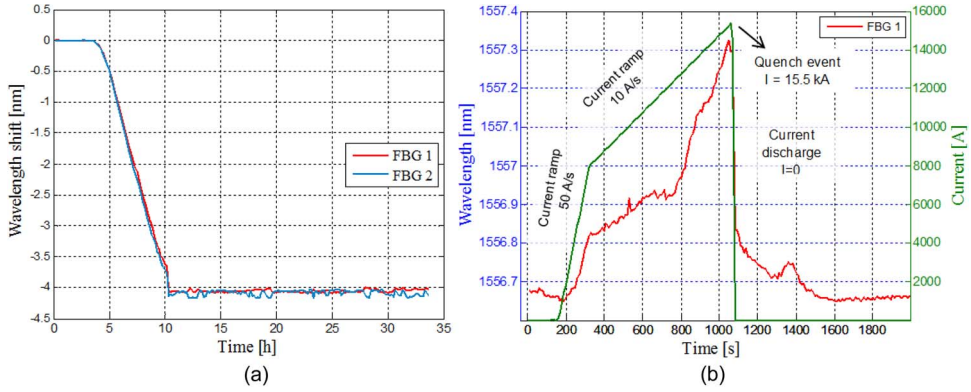

Fig. 10. (a) Wavelength shift during SMC cool down. (b) Embedded FBG response during SMC powering at 1.9 K.

comparison with 1343 pm/$\mu\varepsilon$ measured by the strain gauges. The difference between the strain gauges and the FBGs is due to the different locations on the structure of the magnet which results to be indeed not perfectly symmetric. Moreover the difference between each FBG can be also explained as the result of the different locations as well as the effect of the glue substrate.

Fig. 9(b) summarizes the wavelength shift of the FBGs in the azimuthal direction during the two thermal cycles showing the reliability of the fibers and of the bonding process. After the validation of these results at 77 K the next step will be to study the mechanical behavior of the magnet structure during the cold powering at 1.9 K.

The same assembly procedure was followed for SMC that was then tested during four thermal cycles to 1.9 K and 4.2 K and its training quenches when the magnet is powered each time to higher current up to the quench event. Fig. 10(a) shows the change in wavelength during the cool down from 300 to 1.9 K for the two embedded sensors. As mentioned in Section 2, the response is dominated by the thermal apparent strain induced by the thermal contraction of the host material which explains the blue shift of λ. Despite the complex integration in the coil the fibers survived to four thermal cycles to 1.9 K and 4.2 K showing reproducibility of data and allowing a complete monitoring of the coil mechanical behavior during its operation.

After the cool down, the magnet was powered with current ramped at 50 A/s to 8 kA and then at 10 A/s to the quench current. In response to the powering, the coil releases the pre stress achieved after the assembly and the cool down expanding in its axial direction, while after each quench, when the current is discharged, the coil returns to the original strain it had before the powering. This is illustrated in more details in Fig. 10(b) for FBG1 where the current profile is

also plotted, showing the increase of the wavelength during the ramp followed by a sharp decrease after the quench at 15.5 kA, though the slope variation during the ramp is under further investigation. Moreover the exponential decay of the wavelength after the quench may be explained by the combination of mechanical and thermal effects, these due to the Joule heating in the zone of the quench initiation. In order to study this behavior, a dedicated sensors configuration will be implemented in the next magnet.

The results obtained are in agreement with the expected global behavior of the magnet, but no reference data from strain gauges can be reported in this paper since they resulted to be lost after the first cool down to 4.2 K.

5. Conclusion

An FBG based monitoring system has been implemented for both temperature and strain monitoring in the 20 m superconducting transmission line prototype and in two subscale dipole magnets tested in a range from 300 K to 1.9 K. A multipoint sensing system gives perspective for the implementation of an accurate temperature monitoring over long distances able to preserve the safe working conditions of the superconducting cables. Moreover, the successful implementation proved by a good signal quality and the fiber robustness in the complex environment of high energy physics give perspectives for developing a promising alternative or a complementary instrumentation to the resistive strain gauges in the field of superconducting Nb_3Sn based magnets, specifically during their R&D phase as well as during operation.

Acknowledgment

The authors would like to thank the support of the TF, SCD, and the MDT sections of the TE-MSC group at CERN.

References

[1] L. Bottura, G. de Rijk, L. Rossi, and E. Todesco, "Advanced accelerator magnets for upgrading the LHC," *IEEE Trans. Appl. Supercond.*, vol. 22, no. 3, Jun. 2012, Art. ID. 4002008.
[2] H. Zhang *et al.*, "Development of strain measurement in superconducting magnet through fiber Bragg grating," *IEEE Trans. Appl. Supercond.*, vol.18, no. 2, pp. 1419–1422, Jun. 2008.
[3] C. Lupi, F. Felli, A. Brotzu, M. A. Caponero, and A. Paolozzi, "Improving FBG sensor sensitivity at cryogenic temperature by metal coating," *Sens. J. IEEE*, vol. 8, no. 7, pp. 1299–1304, Jul. 2008.
[4] R. Ramalingam, "Fiber Bragg grating sensors for localized strain measurements at low temperature and in high magnetic field," in *Proc. AIP Conf.*, Nov. 2010, vol. 1218, no. 1, pp. 1197–1204.
[5] A. D. Kersey, "Review of recent developments in fiber optic sensor technology," *Opt. Fiber Technol.*, vol. 2, no. 3, pp. 291–317, Jul. 1996.
[6] S. Gupta, T. Mizunami, T. Yamao, and T. Shimomura, "Fiber Bragg grating cryogenic temperature sensors," *Appl. Opt.*, vol. 35, no. 25, pp. 5202–5205, Sep. 1996.
[7] S. W. James, R. P. Tatam, A. Twin, M. Morgan, and P. Noonan, "Strain response of fibre Bragg grating sensors at cryogenic temperatures," *Meas. Sci. Technol.*, vol. 13, pp. 1535–1539, 2002.
[8] H. Zhang *et al.*, "Fiber Bragg grating sensor for strain sensing in low temperature superconducting magnet," *IEEE Trans. Appl. Supercond.*, vol. 20, no. 3, pp. 1798–1801, Jun. 2010.
[9] R. Rajini-Kumar, M. Suesser, K. G. Narayankhedkar, G. Krieg, and M. D. Atrey, "Performance evaluation of metal-coated fiber Bragg grating sensors for sensing cryogenic temperature," *Cryogenics*, vol. 48, no. 3/4, pp. 142–147, Mar./Apr. 2008
[10] T. Mizunami, H. Tatehata, and H. Kawashima, "High-sensitivity cryogenic fibre-Bragg-grating temperature sensors using Teflon substrate," *Meas. Sci. Technol.*, vol. 12, no. 7, pp. 914–917, Jul. 2001.
[11] J. Roths, G. Andrejevic, R. Kuttler, and M. Süßer, "Calibration of fiber Bragg cryogenic temperature sensors," *Opt. Fiber Sens., OSA Tech. Dig., Opt. Soc. Amer.*, Cancún, Mexico, 2006.
[12] M. Esposito *et al.*, "Fiber Bragg grating sensors to measure the coefficient of thermal expansion of polymers at cryogenic temperatures," *Sens. Actuators A Phys.*, vol. 189, pp. 195–203, Jan. 2013.
[13] M. Bajko *et al.*, "The Short Model Coil (SMC) dipole: An R&D program towards Nb3Sn accelerator magnets," *IEEE Trans. Appl. Supercond.*, vol. 22, no. 3, Jun. 2012, Art. ID. 4002704.
[14] E. Fornasiere *et al.*, "Status of the activities on the Nb3Sn dipole SMC and of the design of the RMC," *IEEE Trans. Appl. Supercond.*, vol. 23, no. 3, Jun. 2013, Art. ID. 4002308.
[15] R. R. Hafalia *et al.*, "A new support structure for high field magnets," *IEEE Trans. Appl. Supercond.*, vol. 12, no. 1, pp. 47–50, Mar. 2002.
[16] S. Caspi *et al.*, "The use of pressurized bladders for stress control of superconducting magnets," *IEEE Trans. Appl. Supercond.*, vol. 11, no. 1, pp. 2272–2275, Mar. 2001.